An Efficient Geometric Integrator for Thermostatted Anti-/Ferromagnetic Models

Teijo Arponen
Institute of Mathematics
Helsinki University of Technology
Finland

Ben Leimkuhler
Department of Mathematics
University of Leicester
U.K.

24th May 2004

Abstract

(Anti)-/ferromagnetic Heisenberg spin models arise from discretization of Landau-Lifshitz models in micromagnetic modelling. In many applications it is essential to study the behavior of the system at a fixed temperature. A formulation for thermostatted spin dynamics was given by Bulgac and Kusnetsov [5], which incorporates a complicated nonlinear dissipation/driving term while preserving spin length. It is essential to properly model this term in simulation, and simplified schemes give poor numerical performance, e.g. requiring an excessively small timestep for stable integration. In this paper we present an efficient, structure-preserving method for thermostatted spin dynamics.

Keywords: Heisenberg ferromagnet, micromagnetics, spin dynamics, Landau-Lifschitz equation, Gilbert damping, thermostats, constant temperature, domain walls, geometric integrator, reversible method

1 Introduction

In recent years geometric integrators have become ubiquitous for numerical treatment of differential equations. By a geometric integrator is meant a numerical method that preserves some known structure of the continuous flow. Geometric integrators are particularly important for long term simulations, as are used in molecular sampling or celestial mechanics. In this paper we consider the application of geometric integration principles for the types of spin dynamics systems that arise frequently in modelling of ferromagnets and anti-ferromagnets. Efficient Lie-Poisson schemes for classical spin dynamics described by the Landau-Lifshitz (LL) equation were studied in [10], and related multisymplectic schemes in [9]. Here we develop and test a geometric integrator for a semi-discrete Landau-Lifshitz-Gilbert (LLG) equation which includes a nonlinear dissipative term. This dissipative system forms the foundation for a more complicated thermostatted model, following the approach of Bulgac and Kusnetsov [5, 2]. We design an effective splitting technique for the full coupled system.

LL and LLG are part of a very active current field of research. Other approaches to these equations can be found in [9, 24, 6, 10, 20, 22, 14, 17], which also provide further references. However none of these articles consider a thermostatted version.

Simulation with the thermostatted version shows fascinating global behavior: the system first arranges into patterns (spin domains) with slowly moving domain walls, then visits a quasi-chaotic state and quickly rearranges itself into completely new spin domains. This kind of transition would not be possible with local interactions only. Here the thermostatting variable is defined in such a way that it has a global character.

A number of recent articles have focussed on the geometric integration of molecular systems in the canonical ensemble [4, 15, 3, 12]. In these articles, the aim has been to work from a Hamiltonian formulation for thermostatted molecular simulation and then to provide a suitable symplectic integrator. The starting point is typically Nosé dynamics, although generalizations are possible.

Since the constant energy Heisenberg spin system is Lie-Poisson, it is natural to seek a Lie-Poisson system to model the action of the thermostat. Unfortunately, the straightforward approach to this problem based on rescaling spin vectors by a scaling variable (analogous to Nosé dynamics) fails since the spin length, rather than the rescaled spin length, remains invariant. While it is possible (with some additional complication, due to the presence of constraints) to develop such a model for the thermostatted Heisenberg system, based on the ideas in [12], it is much different in character from the corresponding molecular dynamics models. Moreover, the Lie-Poisson thermostats add additional complexity in the form of a relatively complex bath model. This method will be considered in future work.

Given these complications, we believe that the best available starting point for geometric integration of thermostatted spin dynamics is the alternative framework of Bulgac and Kusnetsov, based loosely on Nosé-Hoover (NH) dynamics. Like NH molecular dynamics, these formulations sacrifice Hamiltonian structure, while retaining a reversing symmetry. It is unclear the extent to which this loss of structure affects the stability of methods and the ultimate resolution of macroscopic features of the spin model. Although in molecular dynamics it is known that the reversible-only methods are often inferior to their symplectic counterparts [13], it is also well established that NH-type methods are far superior to methods that are neither symplectic nor reversible.

The rest of the paper is organized as follows: in Section 1.1 we review splitting methods and apply them to our models. In Sections 2-4 we present the models and methods in detail. In Section 5 we present numerical results. Finally in Section 6 we present some conclusions and discussion.

1.1 Background: Review of splitting methods

The reader is referred to [16, 18] for a detailed discussion of splitting methods. To briefly describe their basic construction, consider a differential equation $\dot{u} = f(u)$, with flow map $\Phi_{\tau,f}$. If $f = f_1 + f_2$, we have $\Phi_{\tau,f} = \Phi_{\tau,f_1} \circ \Phi_{\tau,f_2} + O(\tau^2)$. If the flows on vector fields f, f_1, and f_2 share a first integral, then the composed map will preserve it as well. In this way, geometric integrators can be developed to preserve general classes of Lie groups. If the vector field is time-reversible, i.e. $f(Ru) = -Rf(u)$ for some linear involution R, then the symmetric concatenation or "Strang Splitting" $\hat{\Phi}_{\tau,f} = \Phi_{\frac{1}{2}\tau,f_1} \circ \Phi_{\tau,f_2} \circ \Phi_{\frac{1}{2}\tau,f_1}$, where f_1, f_2 are reversible vector fields, gives a time-reversible map ($R\hat{\Phi}^{-1}_{\tau,f} = \hat{\Phi}_{\tau,f} \circ R$), which, moreover, provides a second-order approximation of the solution on a finite time interval. As an example, if $H = H(q,p) = T(p) + V(q)$, the leapfrog (Störmer/Verlet) integrator results from the concatenation $\hat{\Phi}_{\tau,H} = \Phi_{\frac{1}{2}\tau,V} \circ \Phi_{\tau,T} \circ \Phi_{\frac{1}{2}\tau,V}$.

The construction of splitting methods for various types of flows, and with various orders of accuracy, is discussed in a number of papers (see, e.g, [25, 21]). Practical splitting-based

geometric integrators have been constructed by mathematicians, chemists and physicists for a wide variety of important applications, including the rigid body, general holonomic constraints, particle accelerator models, and the solar system. Vector field splittings were used in [10] to obtain efficient time-reversible integrators for (undamped) spin systems; it is this fundamental scheme that we have extended in this paper to treatment of dissipative and thermostatted systems.

2 The original Landau-Lifshitz model as a Poisson system

There are several versions of the Landau-Lifshitz equation depending on which forces and fields are taken into account. The version we use here is that of [7], discarding the external and demagnetizing field. (Schemes for more general formulations would build on the work presented here.) The equation can be written in the form:

$$\frac{\partial}{\partial t}S = S \times \nabla^2 S + S \times DS, \tag{1}$$

where $x \in I \times I \subset \mathbb{R}^2$, I an interval, $S(x,t)$ is a unit vector in $\mathbb{R}^3$ representing the classical spin at position x and time t, and D is a diagonal matrix representing anisotropy. Clearly $|S| =$ constant in time:

$$\frac{\partial}{\partial t}|S(x,t)|^2 = 2S(x,t) \cdot \frac{\partial}{\partial t}S(x,t) = 0 \quad \forall x, t.$$

Following the usual practice, we discretize the spatial variable x using second order central differences on a regular lattice as in [10] so that in the discretized system the unit length property is conserved. We then get a Poisson system on a lattice. Without loss of generality we may assume the lattice size to be 1:

$$\begin{aligned} S(x,\cdot) &\mapsto z_{ij}, \\ \nabla^2 S(x,\cdot) &\mapsto z_{i,j-1} + z_{i,j+1} + z_{i-1,j} + z_{i+1,j} - 4z_{ij}, \end{aligned}$$

hence (1) becomes

$$\dot{z}_{ij} = z_{ij} \times (z_{i,j-1} + z_{i,j+1} + z_{i-1,j} + z_{i+1,j} - 4z_{ij}) + z_{ij} \times Dz_{ij}. \tag{2}$$

Observe that the $-4z_{ij}$ term may be omitted. We thus have an $n \times n$ lattice of spins: the variable z_{ij} is on the unit sphere in $\mathbb{R}^3$ for $i, j \in \{1, \ldots, n\}$. The i or j index is zero or $n+1$ at boundaries. Except in the case of periodic boundary conditions, the boundary terms should be viewed as artifacts of discretization, and do not have a counterpart in the continuum case (1). In particular, they are not necessarily of unit length.

By periodic boundary conditions we mean

$$z_{0j} = z_{nj}, \quad z_{i0} = z_{in}. \tag{3}$$

Next we define the Poisson structure matrix. Let us denote

$$z := \left[z_{11}^T \mid z_{12}^T \mid \ \ldots \mid z_{1n}^T \mid z_{21}^T \mid z_{22}^T \mid \ \ldots \mid z_{nn}^T \right]^T,$$

i.e. z is a column vector. For an arbitrary $v =: [a,\, b,\, c]^T \in \mathbb{R}^3$ we write

$$\hat{v} := \begin{pmatrix} 0 & -c & b \\ c & 0 & -a \\ -b & a & 0 \end{pmatrix}, \qquad \hat{v}u = v \times u \quad \forall u.$$

The Poisson structure matrix is defined as the block diagonal matrix

$$J(z) := \begin{pmatrix} \hat{z}_{11} & & & & \\ & \hat{z}_{12} & & & \\ & & \hat{z}_{13} & & \\ & & & \ddots & \\ & & & & \hat{z}_{nn} \end{pmatrix}. \tag{4}$$

Now (2) becomes

$$\dot{z} = J(z)\nabla H(z), \tag{5}$$

if we choose the Hamiltonian H

$$H := -\frac{1}{2}\left(\sum_{i,j} \sum_{(a,b)\in NN(ij)} z_{ij} \cdot z_{ab} + \sum_{i,j} z_{ij}^T D z_{ij} + H_0 \right), \tag{6}$$

where NN refers to "nearest neighbours":

$$NN(ij) = \{z_{i,j-1},\, z_{i,j+1},\, z_{i-1,j},\, z_{i+1,j}\},$$

and H_0 represents the boundaries. For example, if we have zero boundaries ($z_{i0} = 0, z_{0j} = 0, z_{i,n+1} = 0, z_{n+1,j} = 0$), then

$$H_0 := 0,$$

while if we have periodic boundary conditions, then

$$H_0 := \sum_j z_{0j} \cdot z_{1j} + \sum_i z_{i0} \cdot z_{i1}. \tag{7}$$

We can easily extend this to a model to include the both ferromagnetic and antiferromagnetic cases:

$$H := -j_K \frac{1}{2}\left(\sum_{i,j} \sum_{NN} z_{ij} \cdot z_{ab} + \sum_{i,j} z_{ij}^T D z_{ij} + H_0 \right), \tag{8}$$

where j_K is the so called exchange integral [1], assumed constant here, as in [2], and

$$j_K \begin{cases} > 0 & \text{for the ferromagnetic model} \\ < 0 & \text{for the antiferromagnetic model.} \end{cases}$$

For an individual spin at the lattice point (i, j) the equation becomes

$$\begin{aligned} \dot{z}_{ij} &= -j_K z_{ij} \times \left(\sum_{(a,b)\in NN(ij)} z_{ab} \right) - j_K z_{ij} \times D z_{ij} \\ &= z_{ij} \times \nabla H(z), \end{aligned} \tag{9}$$

in both periodic and non-periodic cases. From now on we employ the notation

$$\sum_{NN(ij)} z \quad := \sum_{(a,b)\in NN(ij)} z_{ab}.$$

Lemma 2.1. Any system of the form $\dot{z} = J(z)v(z)$ with (4) and v an arbitrary vector function, conserves the spin lengths in time:

$$|z_{ij}(t)| = |z_{ij}(0)|, \quad \forall i, j, t. \tag{10}$$

Proof.

$$\frac{d}{dt}|z_{ij}|^2 = 2z_{ij} \cdot \dot{z}_{ij} = 2z_{ij} \cdot z_{ij} \times v(z) \equiv 0.$$

□

This gives us useful freedom in modelling. Next, the anisotropy term DS is approximated by an average:

$$Dz_{ij} \mapsto D\frac{1}{4}(z_{i,j-1} + z_{i,j+1} + z_{i-1,j} + z_{i+1,j}). \tag{11}$$

this is sometimes referred to [10] as the *Roberts discretization*. Now (9) becomes

$$\begin{aligned} \dot{z}_{ij} &= -j_K z_{ij} \times M(z_{i,j-1} + z_{i,j+1} + z_{i-1,j} + z_{i+1,j}) \\ &= z_{ij} \times \nabla H(z), \end{aligned} \tag{12}$$

where $M = I + D/4$ is a diagonal matrix and H is modified according to (11).

A Numerical Method

As we noted above, (5) is a Lie-Poisson system whose meaning we briefly recall. Define a bilinear form by

$$\{f, g\}(z) := \nabla f(z) \cdot (J(z)\nabla g(z)),$$

which fulfills the Jacobi identity

$$\{\{f, g\}, h\} + \{\{g, h\}, f\} + \{\{h, f\}, g\} = 0,$$

hence $\{\cdot, \cdot\}$ is a Poisson bracket and J is a Poisson structure matrix. Since J is linear with respect to z, this Poisson structure can be derived from a Lie algebra structure, hence it is called a Lie-Poisson structure.

For a detailed discussion on how to integrate this type of system, see [10]. To summarize that paper, the best available method is to split the vector field in even-odd (or red-black) way:

$$\dot{z}_{ij} = V_1 + V_2, \tag{13}$$

where

$$\begin{aligned} V_1 &= \begin{cases} -j_K z_{ij} \times M \sum_{NN(ij)} z, & i + j \text{ even} \\ 0, & i + j \text{ odd}, \end{cases} \\ V_2 &= \begin{cases} 0, & i + j \text{ even} \\ -j_K z_{ij} \times M \sum_{NN(ij)} z, & i + j \text{ odd}. \end{cases} \end{aligned}$$

Both of these flows can be explicitly solved. For example V_1: for $i + j$ odd $z_{ij}(t) = z_{ij}(0)$. For $i + j$ even, the sum over $NN(ij)$ includes only pairs a, b with $a + b$ odd, hence they

are constants (during V_1). Likewise in V_2 the sum is a constant. Denote the integrator of V_1 by $\hat{\Phi}_{1,t}$ and that of V_2 by $\hat{\Phi}_{2,t}$. That is,

$$\Phi_{1,t} = \exp(tV_1), \quad \Phi_{2,t} = \exp(tV_2).$$

The implemented integrator is a symmetric composition of these exact flows:

$$\hat{\Phi}_t := \Phi_{2,\frac{t}{2}} \circ \Phi_{1,t} \circ \Phi_{2,\frac{t}{2}}. \tag{14}$$

This integrator

- is time reversible
- conserves spin lengths
- preserves energy in the isotropic case ($D = I$),

since $\Phi_{1,t}$ and $\Phi_{2,t}$ do.

3 Dissipated version

It is customary to add a dissipation term to (1). In our case the corresponding dissipated version is derived from (12) and becomes

$$\dot{z}_{ij} = z_{ij} \times \nabla H(z) + \alpha z_{ij} \times z_{ij} \times \nabla H(z), \tag{15}$$

where α is a dissipation constant and the corresponding term is known as the Gilbert damping term.

Clearly (15) can be written more compactly

$$\dot{z} = J\nabla H + \alpha J^2 \nabla H. \tag{16}$$

From Lemma 2.1 it follows that $|z| = 1$ everywhere, i.e. the dissipation does not affect spin lengths. Let us first look at the Gilbert damping term more closely through the equation

$$\dot{z} = \alpha z \times (z \times B), \tag{17}$$

where $z \in \mathbb{R}^3$, and $\alpha \in \mathbb{R}$ and $B \in \mathbb{R}^3$ are constants. Or, more compactly,

$$\dot{z} = \alpha J^2 B.$$

This can be explicitly solved. Put

$$\begin{aligned} v &:= z \cdot B, \\ w &:= z \times B, \end{aligned}$$

then (17) is

$$\dot{v} = \alpha(-C_1 + v^2), \tag{18}$$
$$\dot{w} = \alpha v w, \tag{19}$$
$$\dot{z} = \alpha z \times w, \tag{20}$$

where $C_1 > 0$ constant,

$$C_1 = |z|^2 |B|^2.$$

We can solve for v (we have assumed $|z(0)| = 1$):

$$v(t) = -|B|\frac{\mathcal{E}^2\, C_2 - 1}{\mathcal{E}^2\, C_2 + 1}, \tag{21}$$

where

$$\begin{aligned} \mathcal{E} &:= \exp(\alpha|B|t), \\ C_2 &:= \frac{|B| - v_0}{|B| + v_0}. \end{aligned}$$

Observe that, as $t \to \infty$,

$$\begin{aligned} \alpha > 0 &\Rightarrow v(t) \to -|B| \Rightarrow z, B \text{ become antiparallel,} \\ \alpha < 0 &\Rightarrow v(t) \to |B| \Rightarrow z, B \text{ become parallel.} \end{aligned}$$

Substituting v we can solve for w, which is a scalar function times a constant vector:

$$\begin{aligned} w(t) &= f(t)w(0), \\ f(t) &= \frac{\mathcal{E}(C_2 + 1)}{\mathcal{E}^2 C_2 + 1} \longrightarrow 0 \text{ as } t \to \infty, \text{ if } \alpha \neq 0. \end{aligned}$$

Substituting w we can solve for z:

$$z(t) = \exp(g\hat{w}_0)z(0), \tag{22}$$

$$= \cos(g|w_0|)z_0 + \frac{\sin(g|w_0|)}{|w_0|}w_0 \times z_0, \tag{23}$$

where

$$g \equiv g(t) := -\alpha \int_0^t f(\tau)d\tau = \frac{C^2 + 1}{|B|C}\left(\arctan C - \arctan(C\mathcal{E})\right), \tag{24}$$

$$C := \sqrt{C_2} = \sqrt{\frac{|B| - v_0}{|B| + v_0}}. \tag{25}$$

Here $\exp(g\hat{w}_0)$ is expanded as a Magnus series [11]: the direction of $w(t)$ is constant, hence $g\hat{w}_0$ commutes with its integrals and the Magnus series truncates after the first term. The evaluation of that term is best accomplished by Rodrigues' formula, hence (23).

Evaluating g numerically is a problem because eventually v approaches $\pm|B|$ (physically this means z becomes (anti-)parallel to B) so the C in (24) becomes zero. g itself is not singular, but the expression is difficult to evaluate stably. We used the following Taylor expansions in the implementation. If $||B| - v_0| < 0.0001$,

$$g = -1 + \mathcal{E} + C^2\left(-\frac{2}{3} + \mathcal{E} - \frac{1}{3}\mathcal{E}^3\right) + \mathcal{O}(C^4),$$

and if $||B| + v_0| < 0.0001$,

$$g = 1 - \mathcal{E}^{-1} + C^{-2}\left(\frac{2}{3} - \mathcal{E}^{-1} + \frac{1}{3}\mathcal{E}^{-3}\right) + \mathcal{O}(C^{-4}).$$

A Lyapunov Function

Note that

$$|w|^2 = (z \times B) \cdot (z \times B) = -(B \times z) \cdot (z \times B) = -B \cdot z \times (z \times B) = \frac{-B}{\alpha} \cdot \dot{z} = -\frac{\dot{v}}{\alpha},$$

hence

$$\frac{d}{dt} v = -\alpha |z \times B|^2 \leq 0, \text{ if } \alpha \geq 0.$$

Evidentally, v is a Lyapunov function when α is positive. If $H(z) := Cv = Cz \cdot B$, C a scalar constant, then

$$\frac{d}{dt} H = -\alpha C |z \times B|^2, \tag{26}$$

that is, H is a Lyapunov function iff $\text{sgn}(\alpha C) = 1$. In the next section $\text{sgn}(C)$ chooses between a ferromagnet and an antiferromagnet.

Multiple Spins

Now we continue from (15), which can be written

$$\dot{z}_{ij} = z_{ij} \times (-j_K) M \sum_{NN(ij)} z + \alpha z_{ij} \times z_{ij} \times (-j_K) M \sum_{NN(ij)} z. \tag{27}$$

Recall from the previous discussion that $\alpha < 0$ implies z_{ij} tends to become parallel to

$$(-j_K) M \sum_{NN(ij)} z.$$

This means, see (26), that if $j_K > 0$, then $\text{sgn}(\alpha j_K) = -1$ and energy H is decreasing. In other words, for a ferromagnet, negative α implies damping of energy.

To summarize, a ferromagnetic or antiferromagnetic spin system subject to Gilbert damping will uniformly dissipate energy for appropriate choice of the sign of the damping coefficient. Moreover, a Gilbert-damped system is spin-length conserving.

A Numerical Method

To integrate the damped system, we split the vector field in even-odd way as in the conservative case:

$$\dot{z}_{ij} = V_1 + V_2 + V_3 + V_4, \tag{28}$$

where

$$\begin{aligned}
V_1 &= \begin{cases} -j_K z_{ij} \times M \sum_{NN(ij)} z, & i+j \text{ even} \\ 0, & i+j \text{ odd}, \end{cases} \\
V_2 &= \begin{cases} 0, & i+j \text{ even} \\ -j_K z_{ij} \times M \sum_{NN(ij)} z, & i+j \text{ odd}, \end{cases} \\
V_3 &= \begin{cases} -j_K \alpha z_{ij} \times z_{ij} \times M \sum_{NN(ij)} z, & i+j \text{ even} \\ 0, & i+j \text{ odd}, \end{cases} \\
V_4 &= \begin{cases} 0, & i+j \text{ even} \\ -j_K \alpha z_{ij} \times z_{ij} \times M \sum_{NN(ij)} z, & i+j \text{ odd}. \end{cases}
\end{aligned}$$

Now, all of these flows can be explicitly solved. For example V_1: for $i+j$ odd $z_{ij}(t) = z_{ij}(0)$. For $i+j$ even, the sum over $NN(ij)$ includes only pairs a, b with $a+b$ odd, hence they are constant (during V_1). Likewise in V_2, V_3, and V_4 the sums include only constants.

Hence in V_1 and V_2 we solve

$$\dot{z}_{ij} = z_{ij} \times B, \qquad B \text{ constant}, \tag{29}$$

and in V_3 and V_4 we solve

$$\dot{z}_{ij} = \alpha z_{ij} \times z_{ij} \times B, \qquad B \text{ constant}, \tag{30}$$

which are calculated above. Note that (29), (30) have different constants B. The implemented integrator is a symmetric composition of these exact flows:

$$\hat{\Phi}_t := \Phi_{4,\frac{t}{2}} \circ \Phi_{3,\frac{t}{2}} \circ \Phi_{2,\frac{t}{2}} \circ \Phi_{1,t} \circ \Phi_{2,\frac{t}{2}} \circ \Phi_{3,\frac{t}{2}} \circ \Phi_{4,\frac{t}{2}}, \tag{31}$$

where $\Phi_{i,t} = \exp(t\, V_i)$ are the exact flows.

An important feature of our method is that it dissipates energy when the flow (15) does. This can be seen in the following way: we solve the flows $V_1, \ldots, V_4$ exactly, hence every step in the composition (31) follows the energy of the associated vector field exactly. Now V_1 and V_2 conserve H, and V_3 and V_4 are (weakly) dissipating H. By [19, Theorem 2] our H is conserved by Φ_1 and Φ_2, and Φ_3 and Φ_4 do not increase it. Therefore, the composition Φ_t is (weakly) dissipating H.

4 A Thermostatted Integrator

The purpose of a thermostatted dynamical model is to enable sampling from the canonical ensemble, i.e. maintaining constant average temperature by modelling the effect of a "heat reservoir". In such a model, the system must be allowed to exchange energy with its surroundings. That is, we allow the energy to fluctuate. But, at the same time, we want to keep the spin lengths constant. This will be carried out by modifying the dissipation term introduced in previous sections.

We use the thermostatting term suggested in [2]. Given a parameter T (temperature), we introduce a coefficient α allowed to vary with time: $\alpha = \alpha(t)$ and

$$\dot{\alpha} = -\left(\frac{\kappa}{\mathcal{N}T}\right)^2 \sum_{ij} \left(\mathcal{I} - kT\nabla_{z_{ij}}\right) \cdot \left(z_{ij} \times z_{ij} \times \mathcal{I}\right), \tag{32}$$

where k is Boltzmann's constant which we hereafter take to be 1. $\mathcal{N}$ is number of degrees of freedom, i.e. $\mathcal{N} = 3n^2$ since we have an $n \times n$ square lattice, κ is coupling strength and typically $\kappa \approx \sqrt{\mathcal{N}}$. Here we take $\kappa/\mathcal{N} := 1/n$. $\mathcal{I}$ is given by

$$\mathcal{I} \equiv \nabla_{z_{ij}} H := -j_K M \sum_{NN(ij)} z. \tag{33}$$

The thermostatting variable α has been given the nickname "global demon" [2], so called due to its non-local (hence non-physical) character: it affects all spins simultaneously.

The resulting thermostatted system is

$$\dot{z}_{ij} = z_{ij} \times \mathcal{I} + \alpha z_{ij} \times z_{ij} \times \mathcal{I}, \tag{34}$$

$$\dot{\alpha} = -\left(\frac{\kappa}{\mathcal{N}T}\right)^2 \sum_{ij} \left(\mathcal{I} - T\nabla_{z_{ij}}\right) \cdot \left(z_{ij} \times z_{ij} \times \mathcal{I}\right). \tag{35}$$

It is possible to show that the ferromagnetic system thermostatted using (34),(35) samples from the canonical ensemble. This system also conserves spin length. Finally, one easily demonstrates that these equations are invariant under the simultaneous time-coordinate transformation $t \mapsto -t$, $z \mapsto -z$, $\alpha \mapsto -\alpha$, i.e. the equations are time-reversible.

Thermostatted integrator

To integrate the thermostatted model (34)-(35), we split the vector field in an even-odd way as in Section 2, but including the $\dot{\alpha}$ term:

$$\begin{pmatrix} \dot{z}_{ij} \\ \dot{\alpha} \end{pmatrix} = V_1 + V_2 + V_3 + V_4 + V_5, \tag{36}$$

where V_1, V_2, V_3, V_4 are as in Section 3 (with $\alpha = \alpha_0$ =constant) and

$$V_5 \leftrightarrow \begin{cases} z_{ij} & = \text{ constant}, \\ \dot{\alpha} & = \sum_{ij} \left((z_{ij} \cdot B)^2 - B \cdot B - 2T z_{ij} \cdot B \right). \end{cases} \tag{37}$$

Here we have simplified:

$$B := \mathcal{I} = -j_K \, M \sum_{NN(ij)} z \quad (\text{indep. of } z_{ij}),$$

$$\nabla_z \cdot (z \times z \times B) = \nabla_z \cdot ((z \cdot B)z - B) = 2z \cdot B,$$
$$B \cdot (z \times z \times B) = (z \cdot B)^2 - B \cdot B.$$

In V_5 all terms are constant so the equation with V_5 is trivially solved. But note that the update step of α requires $O(n^2)$ computational work. Finally, we have

$$\hat{\Phi}_t := \Phi_{1,\frac{t}{2}} \circ \Phi_{2,\frac{t}{2}} \circ \Phi_{3,\frac{t}{2}} \circ \Phi_{4,\frac{t}{2}} \circ \Phi_{5,t} \circ \Phi_{4,\frac{t}{2}} \circ \Phi_{3,\frac{t}{2}} \circ \Phi_{2,\frac{t}{2}} \circ \Phi_{1,\frac{t}{2}}, \tag{38}$$

where the $\Phi_{i,t} = \exp(t\, V_i)$ are the exact flows on each of the vector fields.

An important feature of this discretization is that it is time-reversible with respect to the mapping $z \mapsto -z, \quad \alpha \mapsto -\alpha, \quad t \mapsto -t$. This can be seen by recalling from Section 1.1 that if $f(Ru) = -Rf(u)$ for some linear involution R, then the Strang splitting gives a time-reversible map. Here $u := (z, \alpha)$ and $Ru := (-z, -\alpha)$. Applying the rule four times in a row: first to Φ_4 and Φ_5 in the roles of Φ_{τ,f_1} and Φ_{τ,f_2} of Section 1.1, secondly to Φ_3 and $\Phi_4 \circ \Phi_5$ in a similar way, next to Φ_2 and $\Phi_3 \circ \Phi_4 \circ \Phi_5$ and finally to Φ_1 and $\Phi_2 \circ \Phi_3 \circ \Phi_4 \circ \Phi_5$, we get the claim.

5 Numerical results

In all our simulations we used $n = 50$, that is, a 50×50 lattice. We used ferromagnets with anisotropy D =diag$(1, 1, \lambda)$. This is known as "easy plane" or "easy axis" anisotropy, corresponding to $\lambda < 1$ or $\lambda > 1$, respectively.

5.1 Dissipated system

Example 1. In Figure 1 we see evidence of the dissipation of energy. In the top panel, we show the energy, while the bottom panel shows the maximum norm of the discrete Laplacian during each time step. Here we used periodic boundary conditions, $\lambda = 1.1$, $\alpha = -0.5$, and timestep $\Delta t = 0.1$. The initial configuration was random (top left of Figure 2).

The graph of the discrete Laplacian suggests the convergence of the solution to a steady state, as seen in Figure 2, which contains snapshots of the graphs of z-component in the same simulation. The order of the pictures is sequential by row and left to right across rows. Intensity (dark/light) is associated to z-component: black represents the spin-down configuration, white spin-up.

The result shown is typical for this model: the lattice converges to two bands of up and down spins. We also tested zero boundary conditions, in which case the dissipated system typically converged to a single band.

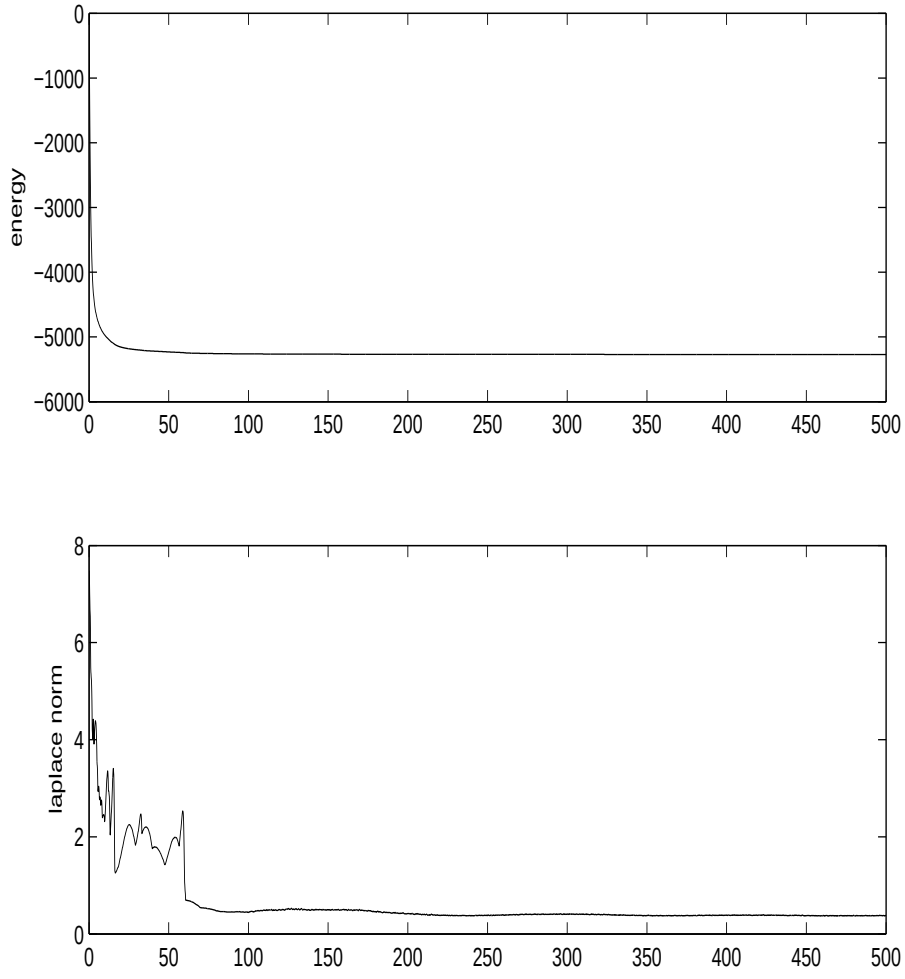

Figure 1: Energy of the dissipated system.

5.2 Thermostatted system

Example 2. In Figures 3 and 4 we diagram the solution of the thermostatted system with periodic boundaries, $\lambda = 0.9$, $T = 0.04$ and timestep $\Delta t = 0.01$. The initial condition

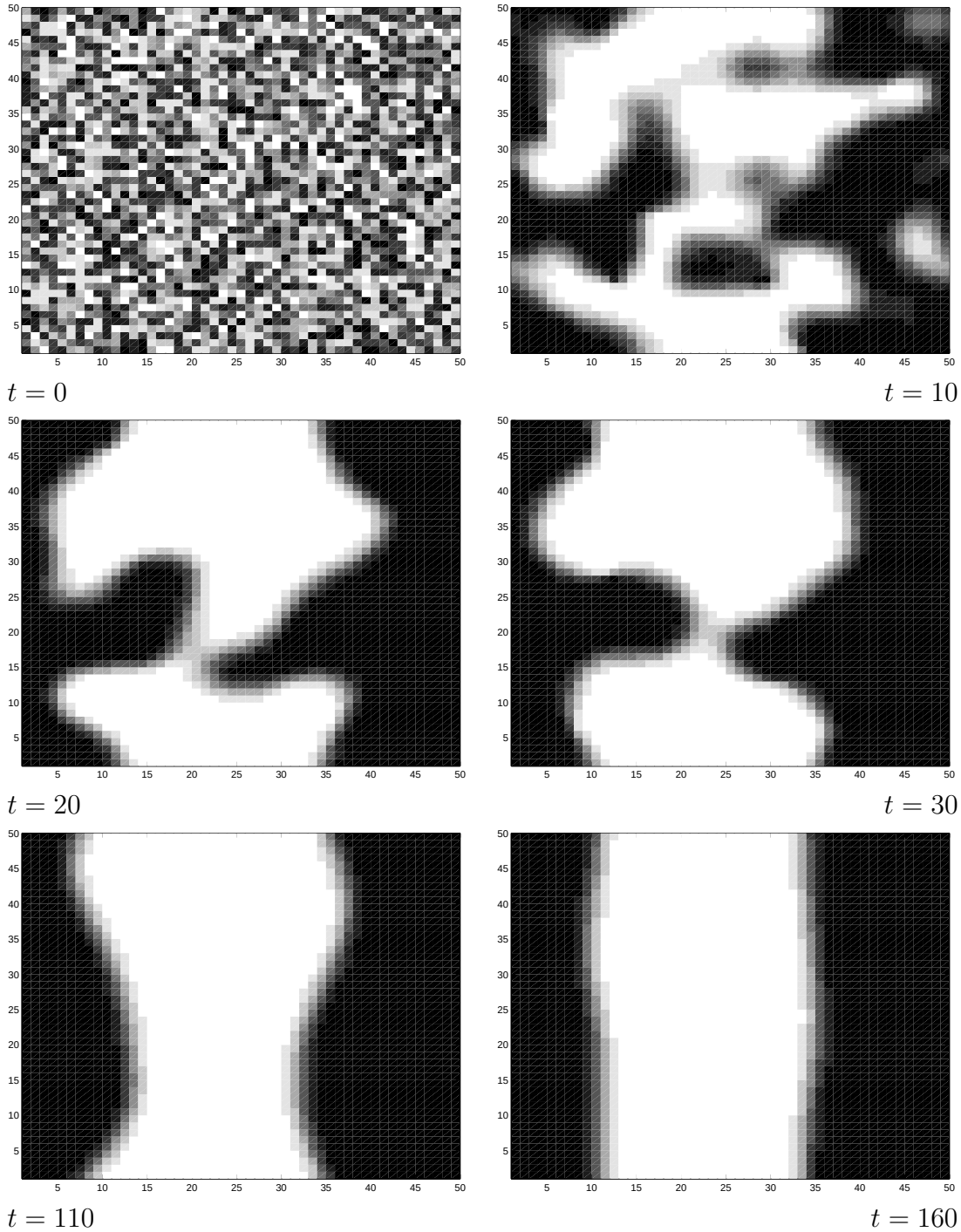

Figure 2: Snapshots of z-components (black: $z = (0, 0, -1)$, white: $z = (0, 0, 1)$) of the dissipated system.

is random. In the top panel of Figure 3, we plot the thermostatting variable α, in the middle panel the energy, and in the bottom panel the maximum norm of the discrete Laplacian. After an initial phase both α and energy settle to an aperiodic oscillatory motion, α between -10 and $+10$, and the energy between -4800 and -4300. We plotted only 2000 steps but the behavior continued similarly for at least 25000 steps. In Figure 4 we can see a slow evolution; the reader is asked to compare the white areas. At $t = 5.2$ the dynamics suddenly appear chaotic, then gradually transition back to a smooth phase. After 25000 steps we still observe slow motion: the system does not converge to any particular formation.

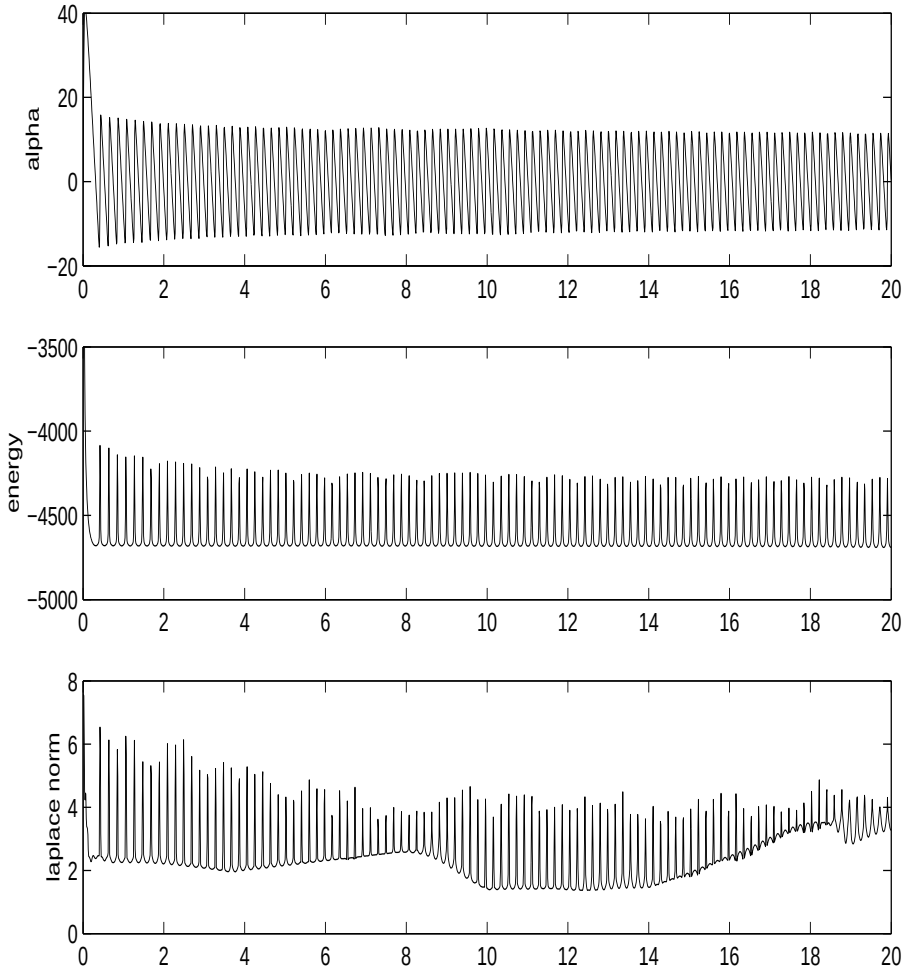

Figure 3: Energy, α, and norm of Laplacian for the thermostatted system of Example 2.

Example 3. As another illustration of the dynamics in this spin model, we exhibit, in Figures 5-9 the numerical solution of the thermostatted system for a system of "wandering vortices". This system has random initial conditions, periodic boundaries, and parameters $\lambda = 0.9$, $T = 0.05$ and timestep $\Delta t = 0.05$. Figures 5 and 6 represent the evolution of α, energy, and averages of the energy over different time windows. Interestingly, the behavior of α is much more erratic than in Example 2. The snapshots in Figures 7-9 show the $z-$components of the lattice. From a random state, the system very quickly forms vortices. The dynamics consists of smooth gyration with brief chaotic interludes as the thermostat variable is driven between positive and negative values. Sometimes the vortices die out completely leaving an apparently smooth surface, but then reappear

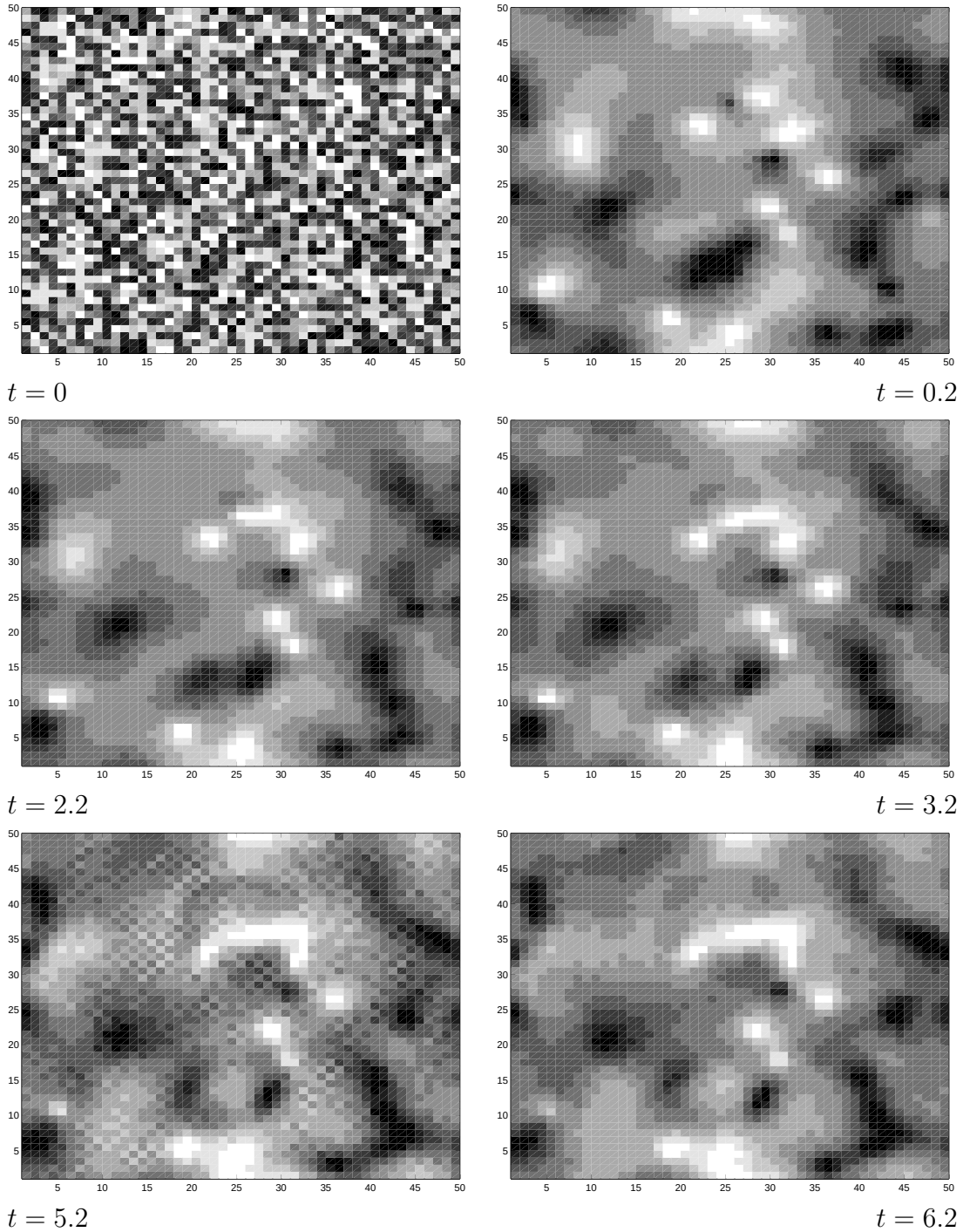

Figure 4: Snapshots of z-components (black: $z = (0, 0, -1)$, white: $z = (0, 0, 1)$) of the thermostatted system in Example 2.

suddenly.

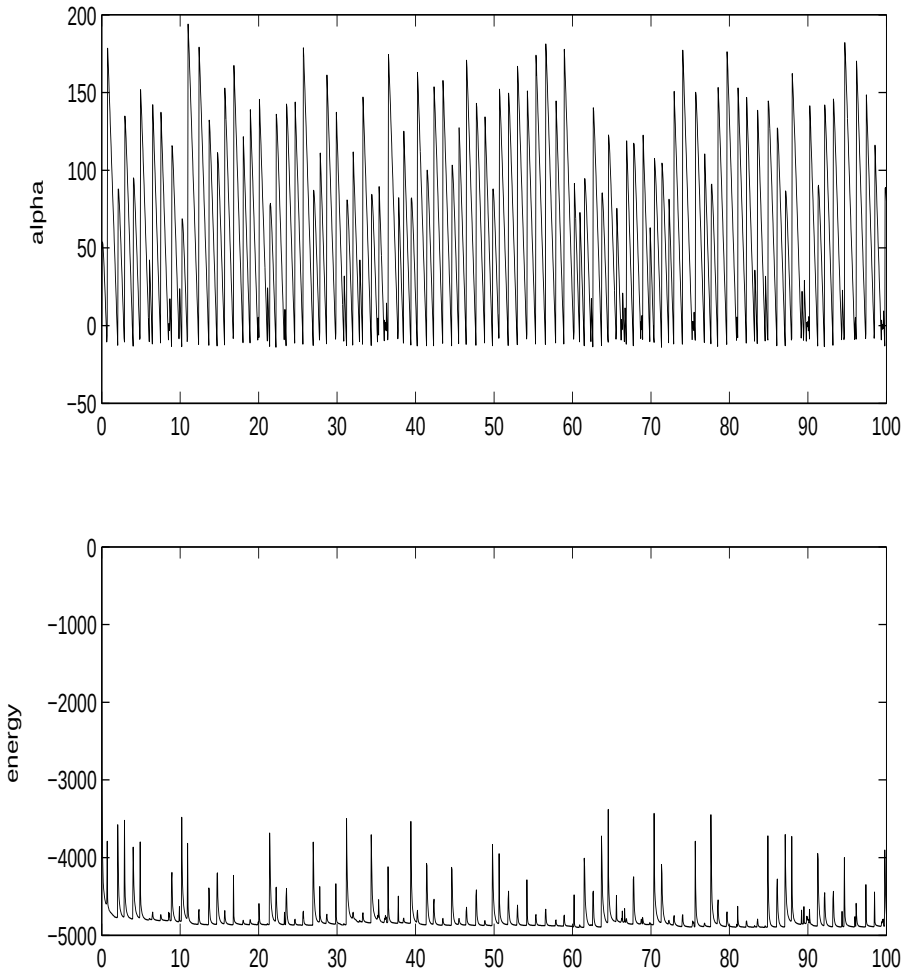

Figure 5: Energy and α of the "wandering vortices", Example 3.

Comparison to RK4 with projection

For comparison we implemented the classical Runge-Kutta 4^{th} order method (RK4) with projection: after every step we normalize

$$z_{ij,new} := z_{ij,RK}/|z_{ij,RK}|,$$

where $z_{ij,RK}$ denotes the result of RK4 step. At very small timesteps for which the RK4 method could successfully integrate the problem, it was slightly faster than splitting, but the RK4 method became rapidly unstable as the stepsize and/or anisotropy were increased. The splitting method was able to handle large anisotropies ($\lambda = 3$) and step sizes ($\Delta t = 0.3$). However, we did not seek the limits of our splitting method. The values $\lambda = 3$ and $\Delta t = 0.3$ indicate the superior stability well enough at this stage.

We tested the projected RK4 on Examples 2 and 3. We kept the other parameters intact but changed the step size. As a sign of failure, we stopped the computation when the code became unstable. In Example 2 the maximum timestep was 0.01, while in Example 3 $\Delta t_{max} = 0.015$. The results are summarized in Table 1.

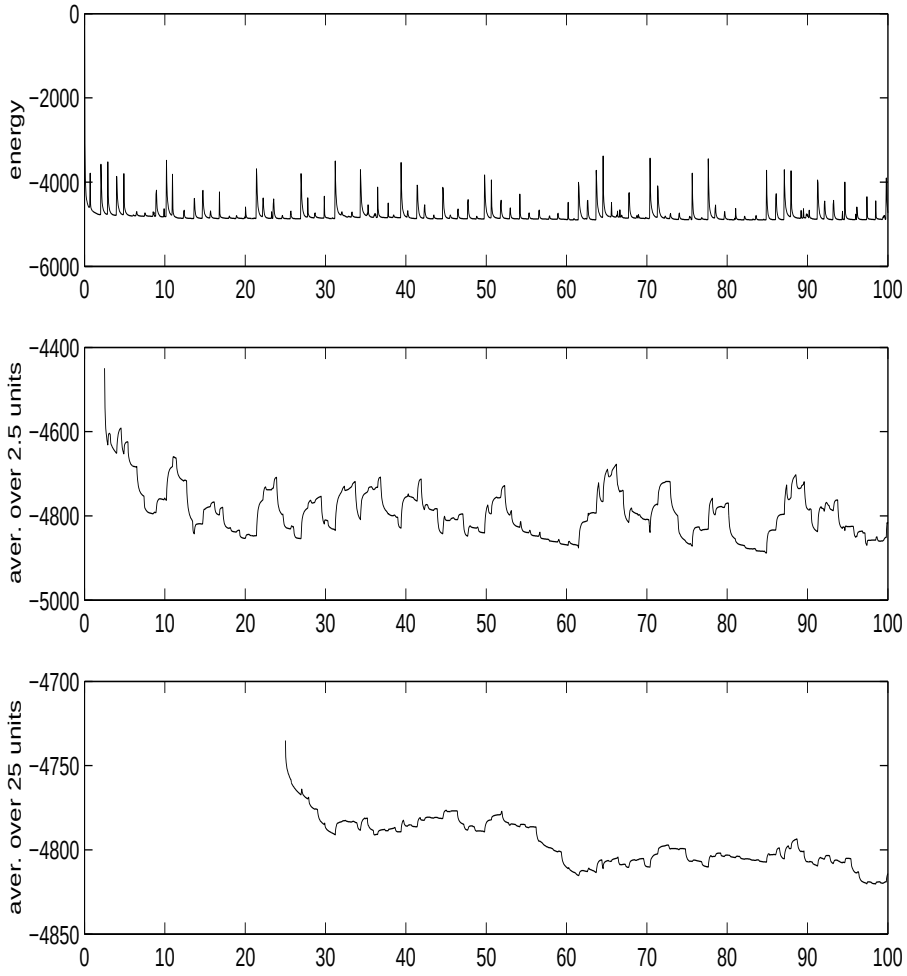

Figure 6: Averages of the energy of the "wandering vortices", Example 3.

6 Discussion

In this paper we have developed and tested a geometric integrator for a semi-discretized Landau-Lifshitz-Gilbert (LLG) equation which includes a nonlinear dissipative term, as well as for a more complicated thermostatted model, following the approach of Bulgac and Kusnetsov.

The integrator for the dissipated system is shown to have a dissipative property. LLG is currently a very active topic of research as mentioned in the introduction. However, it seems that until now there has not been a geometric integrator proposed for the thermostatted system.

Trying to simulate the thermostatted systems with projected RK4 revealed both the features of a stiff ODE and some features of a conservative system. The combination is extremely difficult for standard form numerical methods. The key feature of our splitting method is that it is constructed from composition of building blocks that simulate each of the two components of the system correctly.

Simulation with our new thermostatted method has demonstrated interesting phenomena: slowly creeping boundaries, or wandering vortices, both of which appear from random initial conditions. Our informal term "wandering vortices" in Example 3 refers not to certain particular vortices that survive throughout the whole simulation, but to a

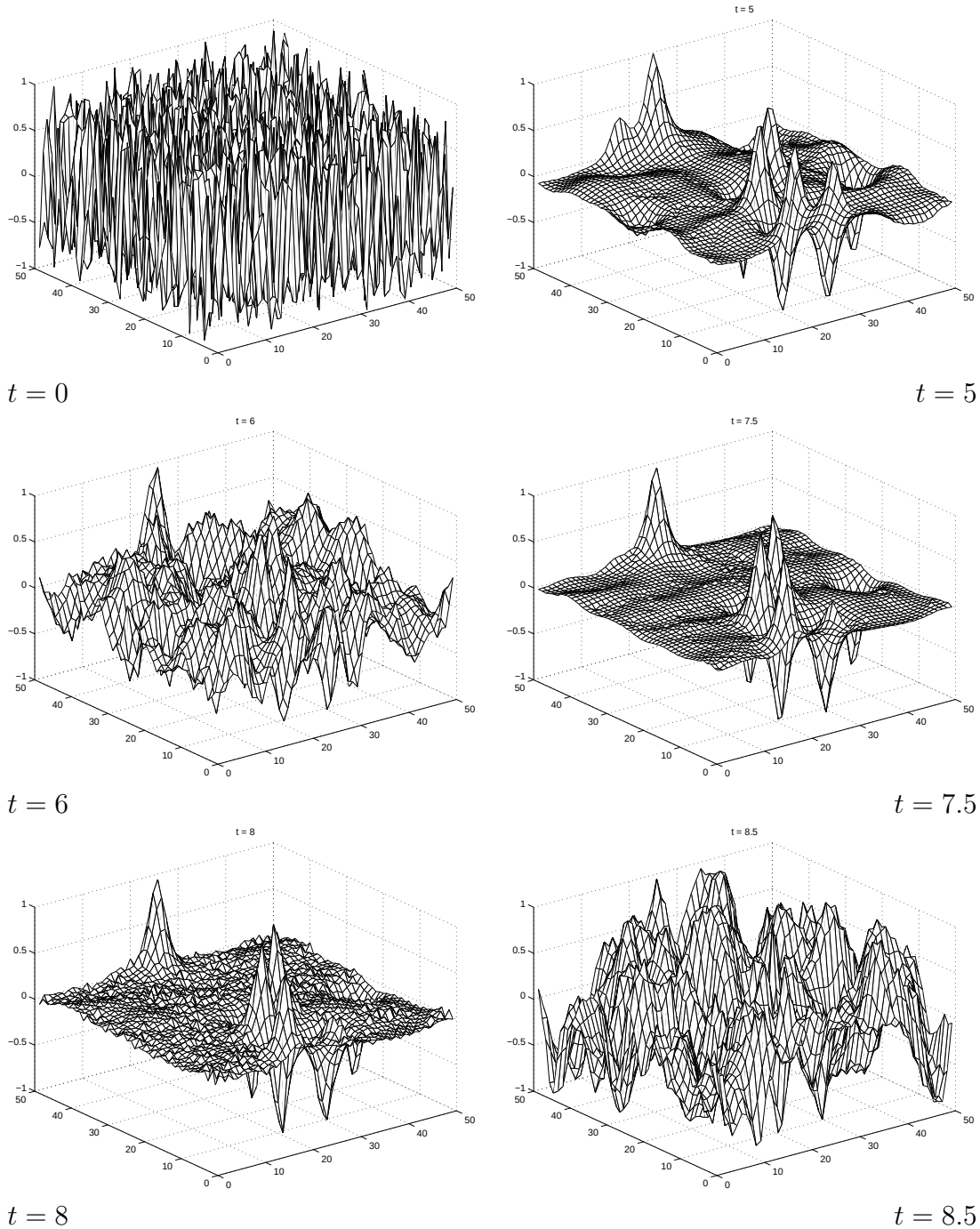

Figure 7: Snapshots of "wandering vortices", Example 3.

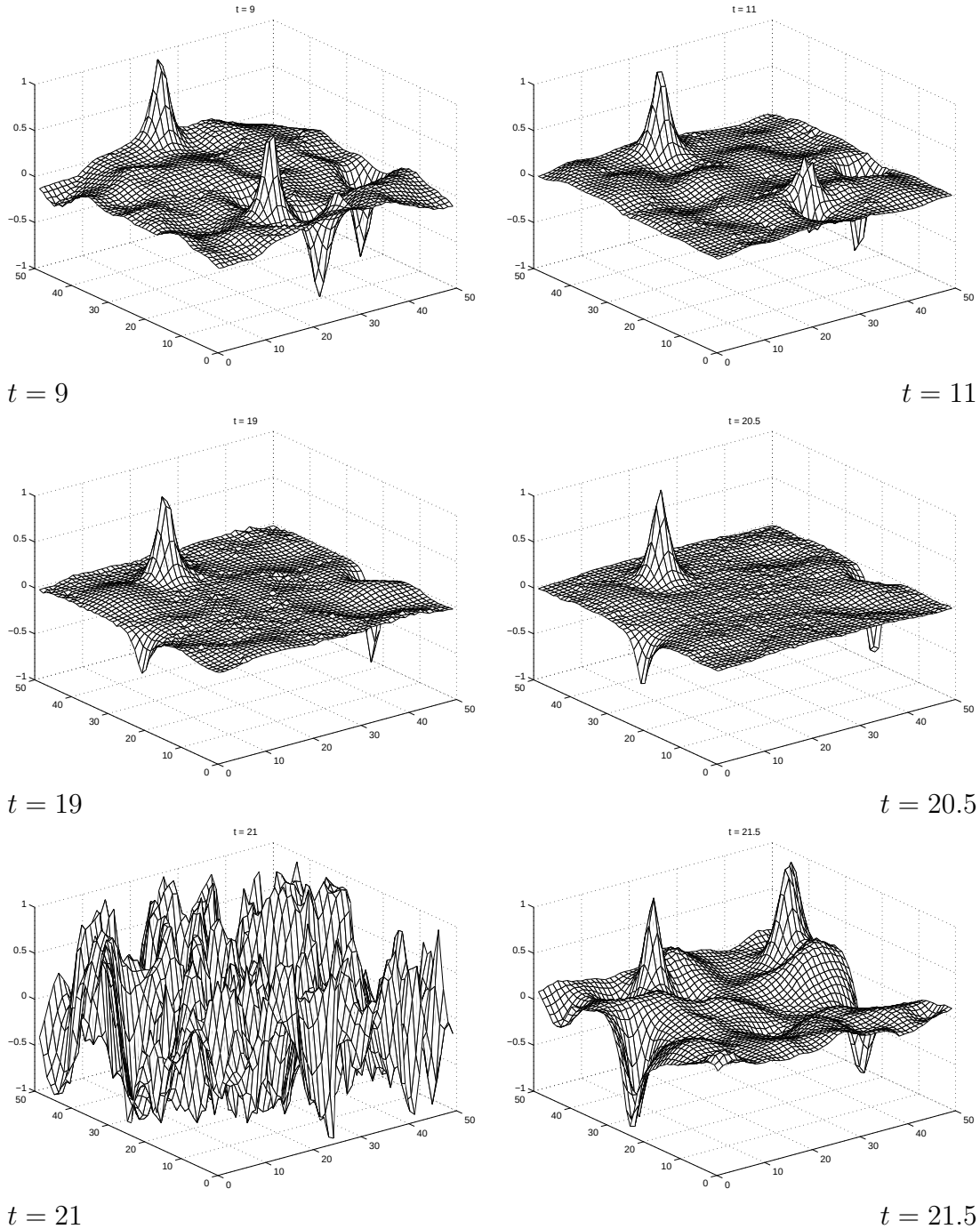

$t = 9$ $t = 11$

$t = 19$ $t = 20.5$

$t = 21$ $t = 21.5$

Figure 8: Snapshots of "wandering vortices", Example 3.

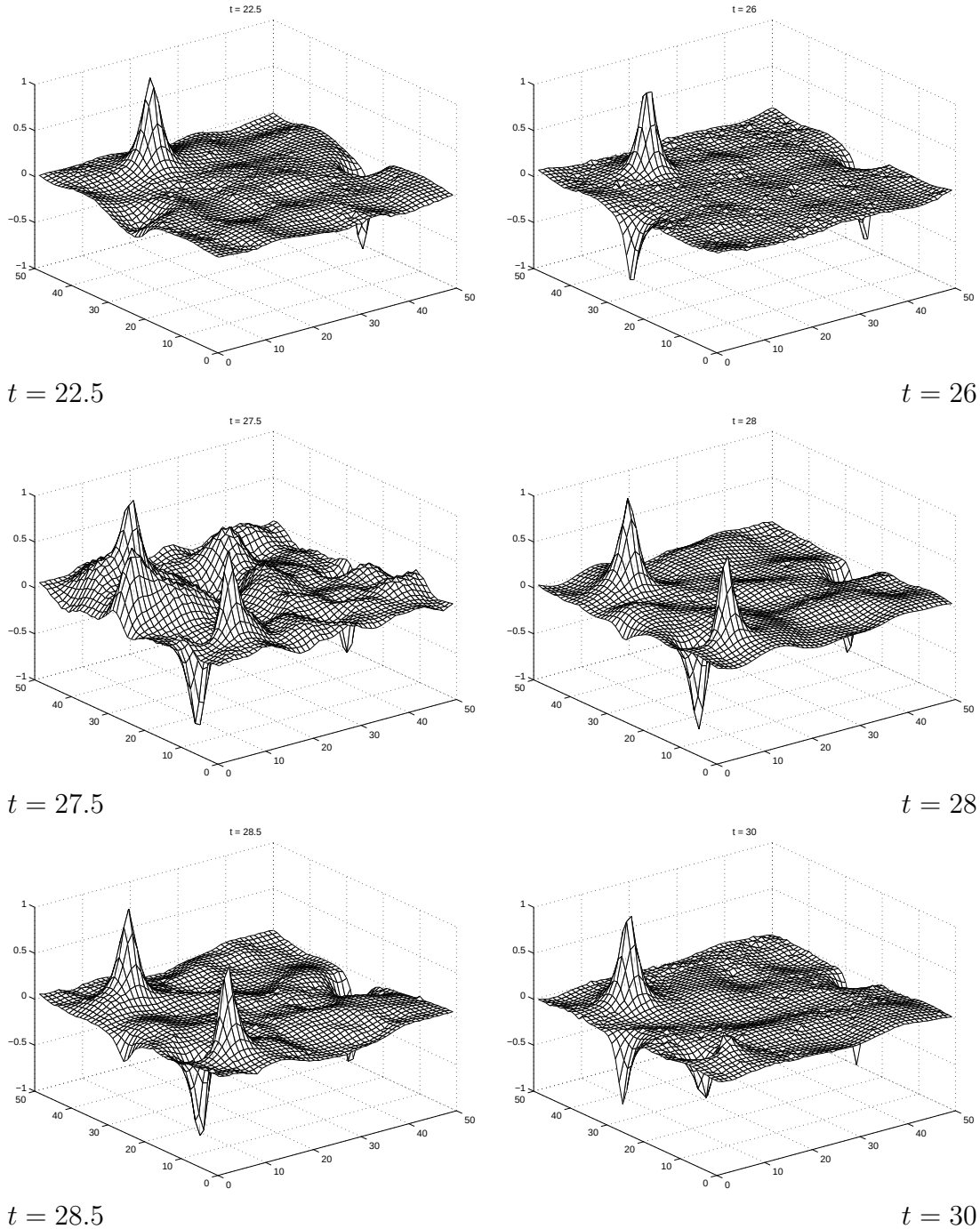

$t = 22.5$ $t = 26$

$t = 27.5$ $t = 28$

$t = 28.5$ $t = 30$

Figure 9: Snapshots of "wandering vortices", Example 3.

Example 2	Δt	RK4 survived up to $t =$
	0.020	0.060
	0.015	0.075
	0.012	0.084
	0.011	0.099
	0.0105	0.116
	0.0102	0.235
	0.010	> 200
Example 3	Δt	RK4 survived up to $t =$
	0.020	0.080
	0.019	0.095
	0.017	0.102
	0.016	0.112
	0.015	> 150

Table 1: Failure of projected RK4.

situation where we have two or more vortices which wander for a while, then violently crash and form new vortices. Intermediate states include a "quasi-chaotic" state, by which we mean a state that suddenly appears and looks random but is not, since it transitions immediately back to (almost) the same smooth motion.

The RK4 method is less stable than the geometric integrator. The stepsize restriction is an order of magnitude more severe compared to our splitting method. This is evidence of stiffness in the ODEs, and a better choice might seem to be a stiff solver on this account, but if one uses a stiff solver the result would be poor resolution of the conservative evolution which is also an important component of the dynamics of the system. The best compromise is therefore a composition scheme, such as that outlined here, which separately and appropriately resolves each term of the system.

We anticipate that this work will stimulate further research in the development of thermostatted numerical methods for systems with complicated nonlinear structure.

Acknowledgements. The authors are grateful to Jason Frank both for valuable comments and providing the code of [10]. The author TA was supported by the Academy of Finland. BL was supported by the Engineering and Physical Sciences Research Council, grant GR/R03259/01. We also wish to thank the referees for their helpful suggestions.

References

[1] J.C. Anderson. *Magnetism and Magnetic Materials*. Chapman and Hall, 1968.

[2] V.P. Antropov, M.I. Katsnelson, B.N. Harmon, M. van Schilfgaarde, and D. Kusnezov. Spin dynamics in magnets: equation of motion and finite temperature effects. *Phys. Rev. B*, 54(2):1019–1035, 1996.

[3] E. Barth, B. Laird, and B. Leimkuhler. Generating generalized distributions from dynamical simulation. *J. Chem. Phys.*, 118, 5759-5768, 2003.

[4] S. Bond, B. Laird, and B. Leimkuhler. The Nosé-Poincaré method for constant temperature molecular dynamics. *J. Comput. Phys.*, 151, 114-134, 1999.

[5] A. Bulgac and D. Kusnezov. Canonical ensemble averages from pseudomicrocanonical dynamics. *Phys. Rev. A*, 42(8):5045–5048, 1990.

[6] W. E and X.-P. Wang. Numerical methods for the Landau-Lifshitz equation. *SIAM J. Num. Anal.*, 38(5):1647–1665, 2000.

[7] L.D. Faddeev and L.A. Takhtajan. *Hamiltonian Methods in the Theory of Solitons*. Springer Series in Soviet Mathematics. Springer, 1987.

[8] X. Feng and P.B. Visscher. Stability and accuracy of Euler and quaternion micromagnetic algorithms. *J. Appl. Phys.*, 91(10):8712–8714, 2002.

[9] J. Frank. Geometric space-time integration of ferromagnetic materials. Technical report, CWI, Amsterdam, the Netherlands, October 2003.

[10] J. Frank, W. Huang, and B. Leimkuhler. Geometric integrators for classical spin systems. *J. Computat. Phys.*, 133, 1997.

[11] E. Hairer, C. Lubich, and G. Wanner. *Geometric Numerical Integration*, volume 31 of *Springer Series in Computational Mathematics*. Springer, 2002.

[12] B. Laird and B. Leimkuhler. Generalized dynamical thermostatting technique. *Phys. Rev. E*, 68, art. 016704, 2003.

[13] B. Laird and J. Sturgeon. Symplectic algorithm for constant-pressure molecular-dynamics using a Nosé-Poincaré thermostat. *J. Chem. Phys.* 112 , 3474–3482, 2000.

[14] D.P. Landau, A. Bunker, H.G. Evertz, M. Krech, and S.-H. Tsai. Spin dynamics simulations – a powerful method for the study of critical dynamics. arXiv:cond–mat 9912375, Center for Simul. Phys., Univ. Georgia, USA, Dec 1999.

[15] B. Leimkuhler. A separated form of Nosé dynamics for constant temperature and pressure simulation. *Comput. Phys. Comm.*, 148, 206-213, 2002.

[16] B. Leimkuhler and S. Reich. *Geometric Integrators in Hamiltonian Mechanics*. Cambridge University Press, 2004.

[17] D. Lewis and N. Nigam. Geometric integration on spheres and some interesting applications. *J. Comp. Appl. Math.*, 151:141–170, 2003.

[18] R. McLachlan and R. Quispel. Splitting methods. *Acta Numerica*, 11:341–434, 2002.

[19] R. McLachlan, R. Quispel and N. Robidoux. Unified approach to hamiltonian systems, poisson systems, gradient systems, and systems with lyapunov functions of first integrals. *Phys. Rev. Lett.*, 81:2399–2403, 1998.

[20] A. Prohl. *Computational Micromagnetism*. Adv. Numer. Math. Teubner, Stuttgart, 2001.

[21] J. M. Sanz-Serna and M. P. Calvo. *Numerical Hamiltonian Problems*. Chapman & Hall, 1994.

[22] M. Slodička and I. Cimrák. Numerical study of nonlinear ferromagnetic materials. *Appl. Numer. Math.*, 46:95–111, 2003.

[23] P.B. Visscher and X. Feng. Quaternion-based algorithm for micromagnetics. *Phys. Rev. B*, 65:104412, 2002.

[24] X.-P. Wang, C.J. García-Cervera, and W. E. A Gauss-Seidel projection method for micromagnetics simulations. *J. Computat. Phys.*, 171:357–372, 2001.

[25] H. Yoshida. Construction of higher order symplectic integrators. *Phys. Lett. A*, 150(5–7):262–268, 1990.